Scientia Iranica, Vol. 4, No. 4, pp 172–176

SCIENTIA
IRANICA

Switching Performance of Metal Base Transistor

R. Faes* and M. Tabandeh[1]

In this paper, the switching performance of Metal Base Transistor (MBT) devices is studied. It is shown that a combination of MBTs with a very low current gain can be used for very high speed logic circuits. The device switching speed depends on its process parameters, as well as its collector current. The dependence of switching speed on the collector current, doping level and length, as well as the base width, is investigated. A sample logic circuit is also proposed and its power consumption, delay, as well as power delay product, is determined.

INTRODUCTION

Demand for high speed and high frequency circuits has always been a driving force in the search for devices capable of operating at higher frequencies and speeds. Metal Base Transistor (MBT), with short base transit time and low base resistance, can offer these characteristics [1-3]. However, the common-emitter current gain of these devices suffers from scattering at the collector-base junction as well as the base region [4]. It falls below unity for the base width of more than a few tens of angstroms [5,6]. In spite of MBT's low current gain, its inherent high speed nature, due to small junction capacitance, small base resistance and low base transit time, justifies the attempt to investigate a suitable circuit configuration and device structure for MBTs leading to fast gates.

In the next section, the effect of device dimensions on the device parameters of MBT will be discussed and, then, its speed performance for different base, collector width and current will be presented. Suitable parameters for a device are obtained to be used in a gate. To present the high speed performance and applicability of MBT devices in logic circuits, a modified ECL logic circuit using MBT is designed and, finally, its performance is evaluated through simulation.

MBT DEVICE PARAMETERS

To obtain the parameters for an MBT device model, a device geometry shown in Figure 1 is assumed. The minimum spacing, as well as the emitter and base contact stripe widths, are taken as L_e. The emitter area is WL_e, where W is the width of the base and emitter contacts. The collector area is $4L_e(L_e + W)$. Base contact is assumed to be a single stripe due to the low resistivity of the base material. If the resistivity of the base material is ρ_b, then the base resistance, r_b, can be calculated as [7]:

$$r_b = 1.5\rho_b \frac{L_e}{WW_b}, \tag{1}$$

where W_b is the base width. This is the intrinsic base resistance, neglecting contact resistance.

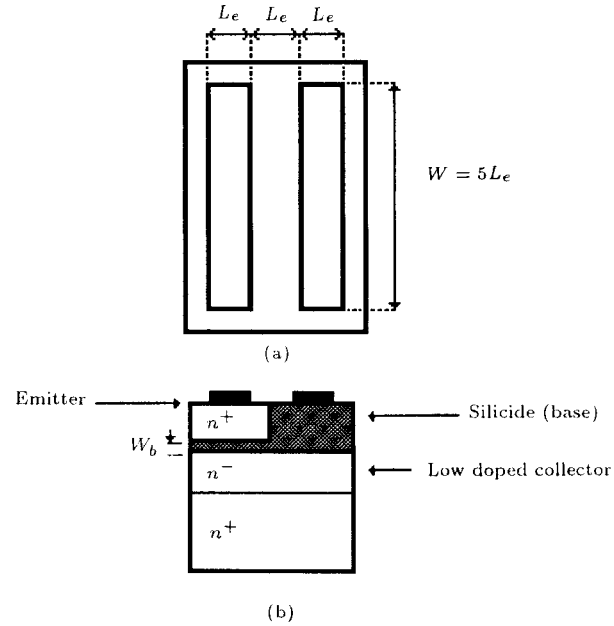

Figure 1. (a) Top view of MBT. The two stripes are emitter and base contacts. (b) Front view of MBT.

* *Corresponding author, Department of Electrical Engineering, Sharif University of Technology, Tehran, I.R. Iran.*

1. *Department of Electrical Engineering, Sharif University of Technology, Tehran, I.R. Iran.*

The emitter resistance is given in [4] as:

$$r_e = \frac{kT}{qL_eWJ_e}, \tag{2}$$

where J_e is the emitter current density obtained from the therminoic emission model. In Equation 2, the effect of the trap recombination in the base-emitter junction is ignored. The source of these traps is the lattice mismatch between metal and semiconductor. This can be reduced by using $CoSi_2$ (or $NiSi_2$), which has a good lattice match with Si and can be grown by MBE [6,8]. MBT is a majority carrier device and, therefore, diffusion capacitance will not be included in the MBT model. The emitter depletion capacitance in terms of current density is given in [4] as:

$$C_e = \{q^2 \in_s N_{de}/2kT\ (1n(\frac{A*T^2N_{de}}{J_eN_c}) - 1)\}^{1/2*}WL_e, \tag{3}$$

where N_{d_e}, N_c and A^* are the doping concentration of emitter, effective density of states in the conduction band and effective Richardson constant, respectively. In the collector area, a low concentration region with a length of L_c adjacent to the base region is assumed. To obtain small collector series resistance, the collector is assumed to be heavily doped next to a low doped region. If the depletion region occupies the whole length of the low doped region, then the following formula can be written:

$$C_c = \in_s \frac{4(L_e + W)L_e}{L_c}. \tag{4}$$

The values of collector capacitance, C_c, as a function of low doped collector length, L_c, and also base resistance, r_b, as a function of base width, W_b, for a device with emitter area of 1 μm × 5 μm, are calculated using Equations 1 and 4 (Figures 2a and 2c). The curves of forward transit time, τ_f, as a function of L_c and the common-base current gain, α, as a function of W_b, derived using Monte-Carlo method [6], are depicted in Figures 2b and 2d.

DEVICE SPEED PERFORMANCE

To optimize the device performance, i.e., increase its speed, it is desired to reduce C_c as well as τ_f and increase α. As shown in Figure 2a, the collector junction capacitance decreases with an increase in the length of its low doped region, L_c . The transit time τ_f, however, increases with L_c due to widening of the collector-base depletion region. Base resistance r_b and the common-base current gain α both decrease with an increase in the transistor base width. These opposing effects suggest that for an optimum device performance in a switching circuit, an MBT must bedesigned to

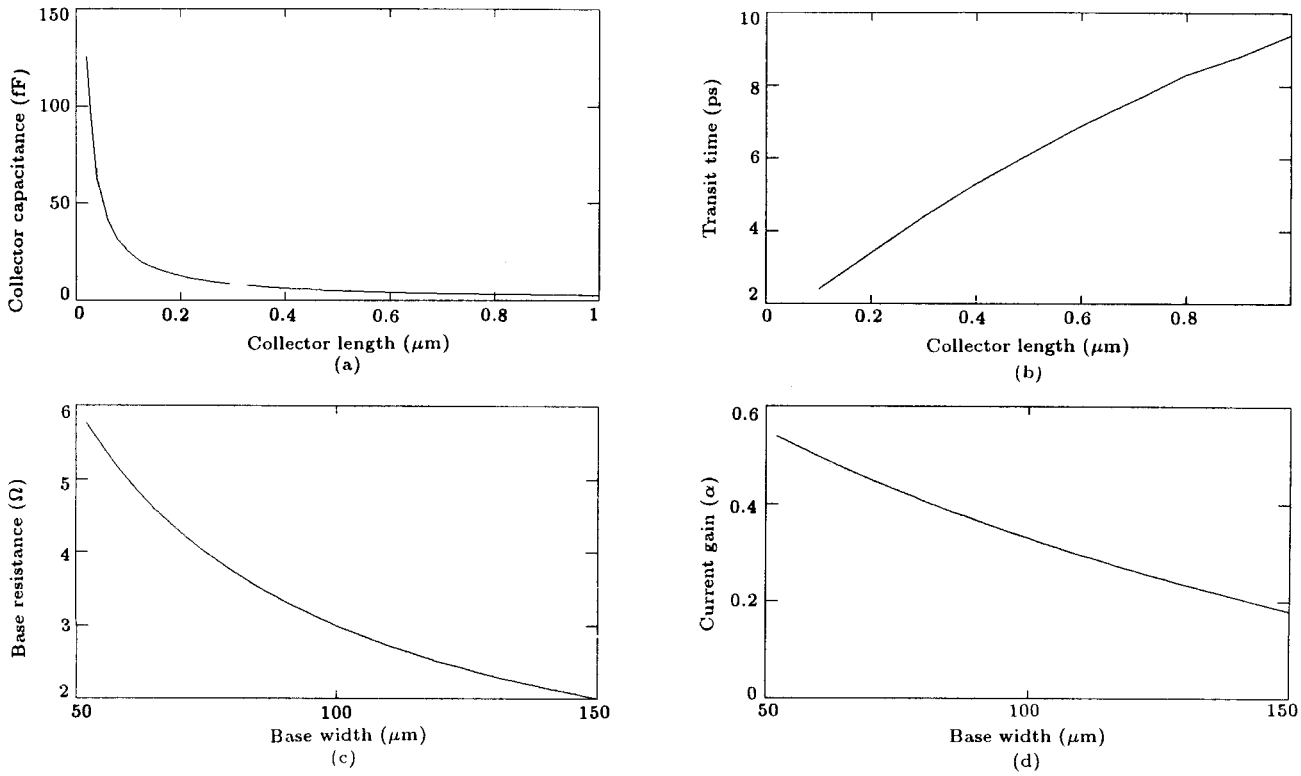

Figure 2. Calculated values of (a) collector junction capacitance C_c, (b) forward transit time τ_f as a function of collector length (L_c) (c) base resistance r_b and (d) common base current gain α as a function of base width.

optimize its circuit performance.

To investigate the effect of changes of the device parameters on its eventual circuit performance, the common-emitter switching behavior of MBT was studied. The propagation delay time for a common-emitter inverter is approximated by Ashar [9] as:

$$t_d = \frac{C_c(R_L + r_b \cdot (1 + R_L/r_e) + r_b C_e}{1 + (1-\alpha) r_b / r_e} + \frac{r_e C_c}{\alpha}. \quad (5)$$

In the above relation, R_L stands for the collector load resistance. Figure 3 shows a plot of t_d vs collector current I_c for different values of the base width W_b,

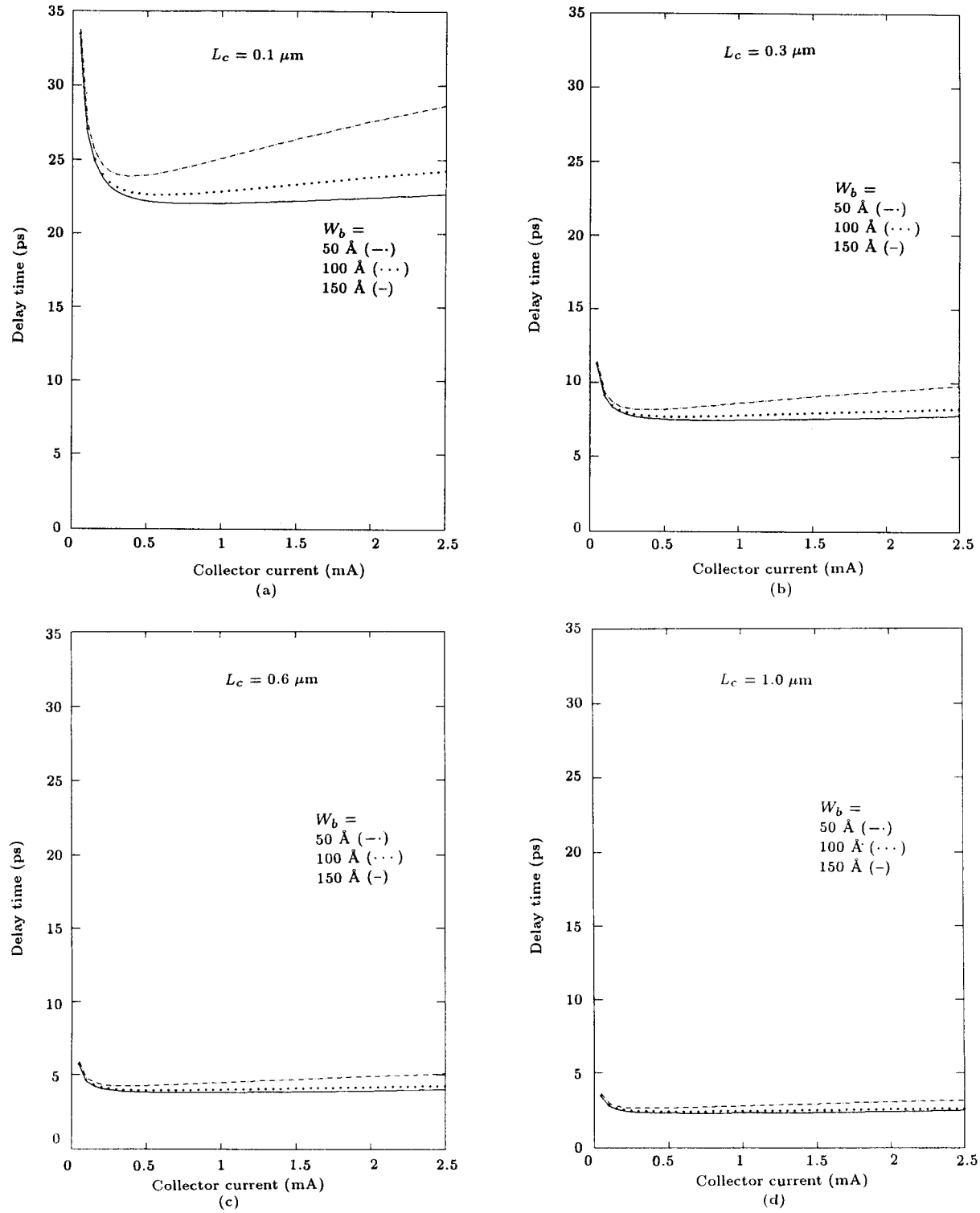

Figure 3. Propagation delay time vs collector current (I_c) for different values of base width (W_b) and low doped collector length (L_c) of (a) 0.1 μm, (b) 0.3 μm, (c) 0.6 μm and (d) 1.0 μm.

using Equation 5 and choosing $R_L = 800\ \Omega$. The reason for choosing the value of R_L will be discussed in the next section. As can be seen in this figure, the propagation delay time changes drastically at low collector current I_c . Therefore, for a given device and for maximum switching speed, the collector current must be calculated in order to yield the best response. However, the collector current at which the maximum speed can be obtained must be less than the current for the onset of high injection. From Figure 3, one can deduce that increasing the length of the low doped collector region will improve t_d. It is to be noted that longer L_c results in higher τ_f but smaller C_c. The propagation delay time t_d, at high enough currents, is dominated by C_c. This is due to the very small base resistance obtainable in MBTs.

A device with the best parameters will now be selected for use in the circuit simulation of the next section. These parameters are those listed in Table 1. Here, due to technical diffqiculty, a value of 100 Å was chosen for MBT base width where, as shown in Figure 2d, the value of the common base current gain of the device for this base width is 0.33.

A LOGIC CIRCUIT USING MBTs

The conventional switching circuit configurations cannot be used directly for these devices, because of the very low common-emitter current gain of MBT. Figure 4 shows a combination of two MBTs with the common-emitter current gain of $\beta < 1$. The effective current gain of a hypothetical transistor equivalent of this combination can be shown to be:

$$\beta_2 = I_{c2}/I_{B1} = \beta(1 + (\beta + 1)) = (1 + \beta)^2 - 1. \tag{6}$$

In general, a combination of n MBTs cascaded in the form of Figure 5 yields an overall current gain of:

$$\beta_n = I_{cn}/I_{B1} = \beta \sum_{k=0}^{n-1} (\beta + 1)^k = (1 + \beta)^n - 1. \tag{7}$$

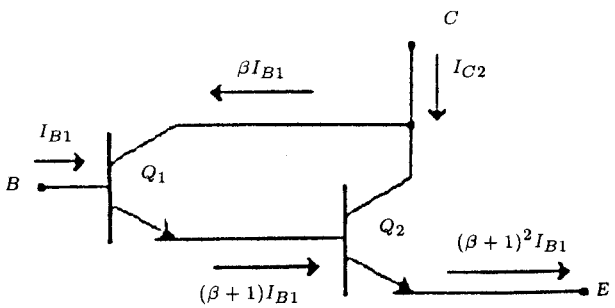

Figure 4. Cascade combination of two MBTs for increasing β.

Thus, for a given value of $\beta < 1$, the number of transistors to be cascaded can be found such that the overall current gain be equal to the number required. This transistor cell of n cascaded transistors can be assumed to be a single device with a common-emitter current gain of $\beta_n > 1$ given by Relation 7, a base-emitter voltage drop of $V_{BEn} = nV_{BE}$ and a minimum collector-emitter voltage of $V_{CESn} = (n-1)V_{BE} + V_{CES}$, where V_{BE} is the base-emitter voltage drop of a single MBT and V_{CES} the collector-emitter voltage for a single MBT at saturation.

A simple ECL type gate similar to that of Figure 6 was chosen as a test vehicle for evaluating the transistor cells as switching devices. The MBT device parameters chosen for the simulation are those listed in Table 1. For the transistor cell of the type shown in Figure 5, in order to have a common-emitter current gain exceeding unity, a minimum of two transistors were required resulting in an overall current gain of $\beta = 1.23$. Using these transistor cells, a nine-stage ring oscillator consisting of the ECL type inverters shown in Figure 6 was simulated using SPICE circuit analysis program. The output waveform shown in Figure 7 presents a propagation delay time of 9.2 ps per gate indicating the high speed performance of MBTs and

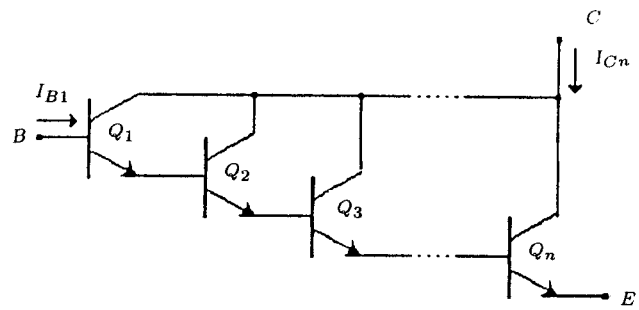

Figure 5. Cascade combination of n MBTs.

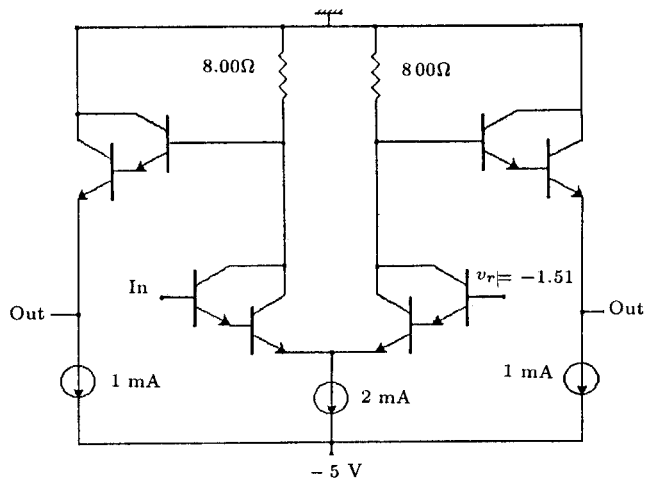

Figure 6. ECL inverter circuit for MBT.

Table 1. Parameters of MBT used in simulations.

Base Material	$CoSi_2$
Base Width W_b	100 Å
Emitter Area	$5 \times 1\mu m$
Low Doped Collector Length	$1.0\mu m$
Minimum Spacing	$1\mu m$
Common-Base Current Gain	0.33
Common-Emitter Current Gain	0.49
Base Resistance r_b	3 Ω
Transit Time τ_f	9.4 ps
Collector Junction Capacitance C_c	2.51 fF

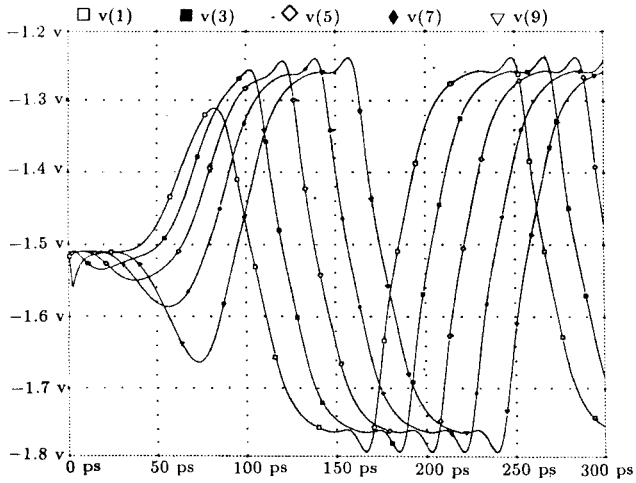

Figure 7. Waveform of a loop oscillator with 9 ECLs.

also their applicability in the logic circuits, in spite of their low current gain. As can be seen from Figure 7, the amplitude of the waveform is 0.5 V for the choice of $R_L = 800\ \Omega$. For higher values of R_L, the amplitude of waveform and also the propagation delay time will increase.

As Figure 6 shows, the total current per gate is 4 mA and voltage source is 5 V. Therefore, the power delay product for this inverter will be 184 fJ. The circuit of Figure 6 is primitive and different cases should be considered to obtain an optimized gate. This will be done in a separate paper as the aim here is only to show how the high speed property of MBT can be used in a logic circuit.

CONCLUSION

Although MBT devices suffer from very low current gain, it was shown that a combination of these devices can be used for very high speed logic circuits using proper circuit configurations. The switching speed of the MBT logic circuits is predicted to be in the range of picoseconds, which proves that MBT is an excellent candidate for very high speed logic circuits.

The maximum switching speed of the device is obtained at a certain collector current, I_{cm}, defined by the device parameters. It was shown that the switching speed increases for wider base widths. The only shortcoming of these devices is their low current gain (β); this can be overcome by choosing a proper number of transistor stages to be cascaded.

REFERENCES

1. Rose, A., Interim Rept. No. 6A, RCA, 1960 ; Govt. Contract Rept. No. bsr 77523 (1960).
2. Attalla, M.M. and Kahng, D. "A new hot electron triode structure", *the Solid State Devices Research Conference*, Durham, N.H. (1962).
3. Geppert, D.V., *Proc. IRE 50*, p 1527 (1962).
4. Sze, S.M. and Gummel, H.K. "Appraisal of metal-semiconductor transistors", *Solid State Elect.*, **9**, p 751 (1966).
5. Abdeshaah, R. and Wang, K.L. "Transport study in si-silicide-si transistors using a Monte Carlo technique", *IEEE Tans. Elect. Dev.*, ED-31, p 1701 (1984).
6. Rosencher, E., Badoz, P.A., Pfister, J.C., Arnaud d'Avitaya, F., Vincent, G. and Delage, S. "Study of ballistic transport Si-$CoSi_2$-Si metal base transistors", *Appl. Phys. Lett.*, **49**, p 271 (1986).
7. Early, J.M., *Proc. Inst. Radio Engrs.*, **46**, p 1924 (1958).
8. Tung, R.T., Gibson, J.M. and Levei, A.F. "A growth strained-layer semiconductor-metal-semiconductor heterostructures", *Appl. Phys. Lett.*, **48**, p 1264 (1986).
9. Ashar, K.G. "The method of estimating delay in switching circuits and the figure of merit of a switching transistor", *IEEE Trans. on Elect. Dev.*, ED-11, p 497 (1964).

Scientia Iranica, Vol. 4, No. 4, pp 177–182

SCIENTIA
IRANICA

Research Note

Coordination of Large-Scale Systems with Fuzzy Interaction Prediction Principle

N. Sadati[1]

Coordination is one of the fundamental issues in multi-level large-scale systems. In this paper, a new approach for coordination by fuzzy set theory based on interaction prediction principle is developed. Infimal control problems are solved within the framework of fuzzy optimal control problems (FOC). Fuzzy coordinator simulates a fuzzy prediction, namely $\tilde{\alpha}$, of the interface inputs. The infimal control units receive the fuzzy prediction and solve an FOC problem to obtain the value of the prediction, i.e., $\hat{\alpha}$. Error ε, between $\hat{\alpha}$ and actual interface inputs $u(\hat{\alpha})$, and also the rate of change of interface inputs are considered as the input fuzzy sets for the coordinator.

INTRODUCTION

The concept of coordination is introduced within the framework of a two-level system shown in Figure 1. The system consists of n infimal (i.e., first-level) controllers denoted by $\mathbf{C_1}, \ldots, \mathbf{C_n}$ involved in the direct control of the process and one supremal (i.e., second-level) controller denoted by $\mathbf{C_0}$ whose decision affects the infimal controllers. The supremal controller objective is to influence the infimal controllers so that a given overall objective, an objective specified for the entire system as a unit, is achieved. This is referred to as coordination [1,2].

Let an overall process $P : M \rightarrow Y$ and a performance function $G : M \times Y \rightarrow V$ be given with M, the set of controls, Y, the set of outputs and V, the set of performance values. Let g be defined on M by the following equation:

$$g(m) = G[m, P(m)]. \tag{1}$$

Now, the goal of the overall control problem, denoted by $\mathcal{D}$, is to find a control action m in M which minimizes g over M ; such a control action will be referred to as the overall optimum.

Let $M = M_1 \times \cdots \times M_n$ and $Y = Y_1 \times \cdots \times Y_n$. For each $i = 1, \ldots, n$, the subprocesses $P_i : M_i \times U_i \rightarrow Y_i$ are given, with U_i the set of interface inputs, such that when intercoupled, as shown in Figure 2, they form the overall process. For each $i = 1, \ldots, n$, the mapping $H_i : M \times Y \rightarrow U_i$ demonstrates the interface input appearing at the ith subprocess in the coupled system. The ith infimal control problem is formulated based on an objective function g_i given on $M_i \times U_i$ in terms of the ith subprocess and a performance function $G_i : M_i \times U_i \times Y_i \rightarrow V$ by the following equation:

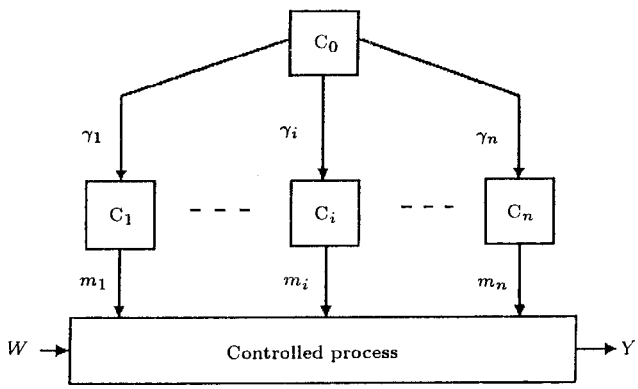

Figure 1. A two level system with n first level controller.

$$g_i(m_i, u_i) = G_i[m_i, u_i, P_i(m_i, u_i)]. \tag{2}$$

As stated in [2], one case that arises regarding how coordination might be affected and the infimal control problems can be defined is model coordination.

Let $U = U_1 \times \cdots \times U_n$. Each $\alpha = (\alpha_1, \ldots, \alpha_n)$ in U for $i = 1, \ldots, n$ provides the subprocesses model

1. *Intelligent Systems Laboratory, Department of Electrical Engineering, Sharif University of Technology, Tehran, I.R. Iran.*

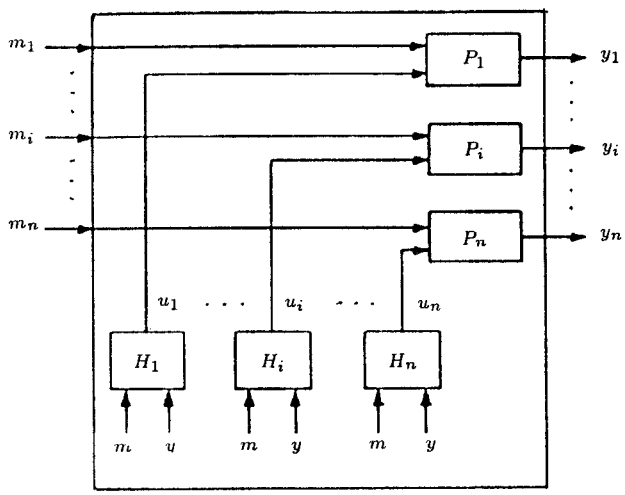

Figure 2. Decomposition of the overall process P.

$P_{i\alpha}(m_i) = P_i(m_i, \alpha_i)$. Subsequently, for each α in U, the infimal control problem $\mathcal{D}_i(\alpha)$ is to find a control $\hat{m}_i$ in M_i such that

$$g_i(\hat{m}_i, \alpha_i) = \min_{M_i} g_i(m_i, \alpha_i). \tag{3}$$

Interaction Prediction Principle

Let $\alpha = (\alpha_1, \ldots, \alpha_n)$ be the predicted interface inputs and $u_1(\alpha), \ldots, u_n(\alpha)$ the actual interface inputs occurring when the control $\hat{m}(\alpha) = [\hat{m}_1(\alpha), \ldots, \hat{m}_n(\alpha)]$ is implemented. The overall optimum is then achieved if the predicted interface inputs are correct, i.e.,

$$\alpha_i = u_i(\alpha) \text{ for all } i = 1, \ldots, n. \tag{4}$$

If the interaction prediction principle applies, it immediately yields that the supremal control problem $\mathcal{D}_0$ is to find $\hat{\alpha} = (\hat{\alpha}_1, \ldots, \hat{\alpha}_n)$ in U such that $\varepsilon_i = \hat{\alpha}_i - u_i(\hat{\alpha}) = 0$ for each $i = 1, \ldots, n$. Alternatively, if ε_i can not be made zero, the supremal control problem can be defined as minimization of an appropriate function f of the errors $\varepsilon_1, \ldots, \varepsilon_n$.

FUZZY COORDINATION

The basic concept of fuzzy coordination is shown in Figure 3. The fuzzy coordinator consists of fuzzy rules which perform functions on incoming input fuzzy sets, namely error signals, as well as the rate of change of interface inputs. The output fuzzy sets, $\tilde{\alpha}_i$, are fuzzy interaction predictions. Hence, the goal of the supremal control problem $\mathcal{D}_0$ is to find fuzzy sets that are good approximations for $u_i(\hat{\alpha})$.

The infimal control problems can be considered as FOC (Fuzzy Optimal Control) problems that are introduced in [3]. Hence, the infimal control problems, $\mathcal{D}_i(\alpha)$, are formulated in the following way.

Find a control action, $\hat{m}_i$ in M_i, such that:

$$g_i(\hat{m}_i, \tilde{\alpha}_i) = \underset{M_i, \tilde{\alpha}_i}{FOC} g_i(m_i, \tilde{\alpha}_i). \tag{5}$$

Note that $\tilde{\alpha}_i$ is a fuzzy set near to crisp whose membership function, $\mu(\hat{\alpha}_i)$, is chosen to have a configuration of Figure 4.

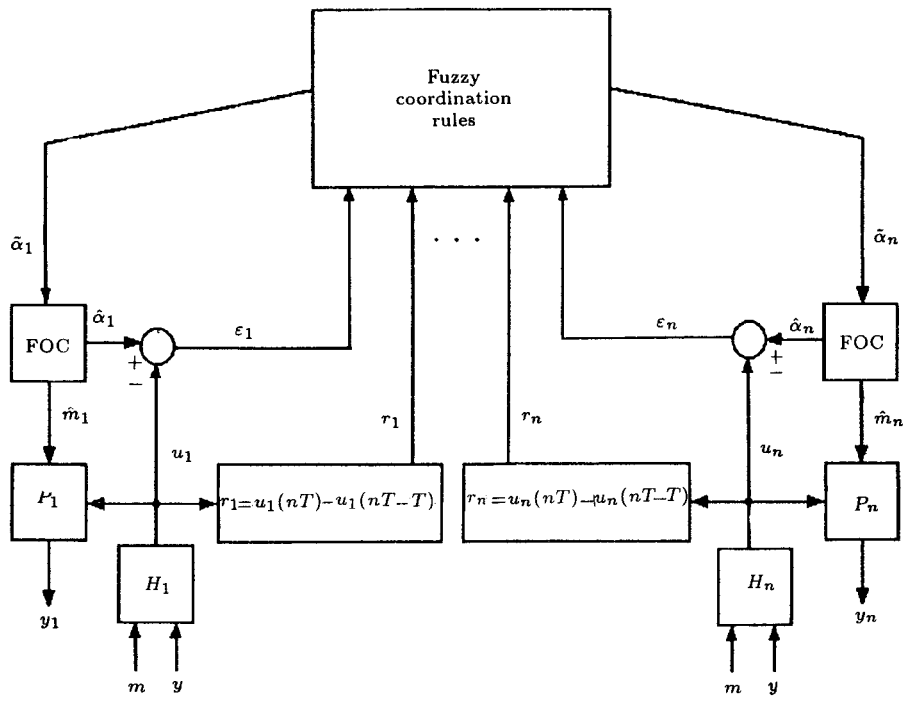

Figure 3. Fuzzy coordination diagram.

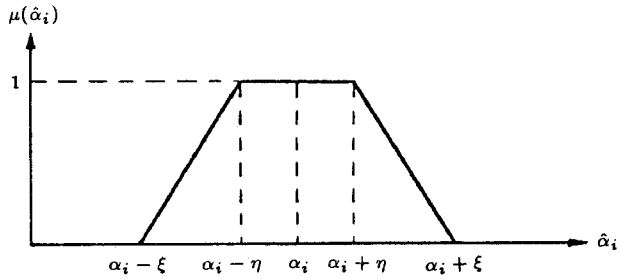

Figure 4. Membership function of $\tilde{\alpha}_i$.

In most cases there are uncertainties on constraints, final conditions, dynamic equations, system parameters and so on. These problems are solved by considering the uncertainties under fuzzy sets, whose membership functions are μ_j for $j = 1, \ldots, q$ [4]. Therefore, the crisp equivalent problem can be formulated as:

$$\max_{M_i, \tilde{\alpha}_i} \lambda$$

subject to:

$$\text{crisp constraints}, \lambda \leq \mu(\alpha_i), \lambda \leq \mu_j; \quad j = 1, \ldots, q.$$

The above optimization problem can be solved to uniquely determine $\hat{m}_i(\hat{\alpha}_i)$ and $\hat{\alpha}_i$. It should be noted that the value of $\hat{\alpha}_i$ is the best member of prediction of fuzzy sets $\tilde{\alpha}_i$ that gives local optimization. Hence, the following principle is proposed.

Fuzzy Interaction Prediction Principle

Let $\tilde{\alpha} = (\tilde{\alpha}_1, \ldots, \tilde{\alpha_n})$ be the fuzzy predicted interface inputs and $\hat{\alpha} = (\hat{\alpha}_1, \ldots, \hat{\alpha}_n)$ the solution of the FOC problems. Also, let $u_1(\alpha), \ldots, u_n(\alpha)$ be the actual interface inputs occurring when the control $\hat{m}(\alpha) = [\hat{m}_1(\alpha), \ldots, \hat{m}_n(\alpha)]$ is implemented. The overall optimum is then achieved if $\hat{\alpha}_i = u_i(\alpha)$ for $i = 1, \ldots, n$.

SPECIFICATION OF FUZZY RULES AND FUZZY SETS

In order to illustrate how fuzzy inference can be used by the coordinator to compute the proper control actions, at any given sampling instance, consider the incoming fuzzy signals of the following form:

$$\varepsilon_i = u_i(nT) - \hat{\alpha}_i(nT), \quad r_i = u_i(nT) - u_i(nT - T), \tag{6}$$

where ε_i and r_i represent the instantaneous values of the error and the rate of change at the nth sampling instants, respectively. It is also assumed that ε_i and r_i, $i = 1, \ldots, n$, take their values on their respective domains of definition E and R. Moreover, let $E = \{E_j\}$ and $R = \{R_j\}$, where $j = -k, -k+1, \ldots, 0, 1, \ldots, k$, is defined on E and R such that a total number of $2k+1$ members for fuzzy sets ε_i and r_i of each subprocess is formed. Furthermore, E_0 and R_0 are centered at the origin of E and R. The membership functions defined on a universe of discourse X, corresponding to E and R, are expressed as:

$$\{\mu_{-k}(x), \ldots, \mu_{-1}(x), \mu_0(x), \mu_1(x), \ldots, \mu_k(x)\}, \tag{7}$$

λ_i is the center value of $\mu_i(x)$, where the linguistic term that it represents fully achieves its meaning, i.e., $\mu_i(x) = 1$. Also, let $\lambda_{-k} = -L$, $\lambda_0 = 0$ and $\lambda_k = L$. Assuming that the space, s, between the central values of two adjacent members is equal, it is easy to see that $s = L/K$ and $\lambda_i = i.s$. Furthermore, it is obvious that the base of each member is $2s$. It should be noted that the equality of the bases does not imply loss of generality because through scaling the inputs, ε_i and r_i, the equality of the bases can be achieved. The membership function, $\mu_i(x)$, of the associated input fuzzy sets is chosen to be triangular shaped (see Figure 5). In a similar manner, $2J + 1$ identical members are assumed, A_j, in the output fuzzy set, "$\Delta\alpha_i$", where $j = -J, \ldots, 0, 1, \ldots, J$. A_0 is centered at the origin of X; furthermore A_j is positive for $j > 0$ and negative otherwise. For each "$\Delta\alpha_i$", the members of the output fuzzy set and corresponding membership functions are defined as follows:

$$\{\mu'_{-J}(x), \ldots, \mu'_0(x), \ldots, \mu'_J(x)\}$$

$$\{A_{-J}, \ldots, A_0, \ldots, A_J\}. \tag{8}$$

Now, choosing γ_i as the central value of the members ($\gamma_J = H$ and $\gamma_{-J} = -H$) and $v = H/J$ as the space between the central values of two adjacent members, the ith central value can be written as $\gamma_i = i.v$.

Membership functions of the associated output fuzzy set are identical to the inputs and can also be shown by Figure 5.

Assuming the rate of change to be approximately linear, as shown in Figure 6, and using points A and B, point C can be depicted as a good prediction of u_i. To demonstrate this, let $\Delta = r - e$, then the predicted value of $u_i(nT + T)$ can be given by $\alpha_i(nT + T) = \Delta + \alpha_i(nT)$.

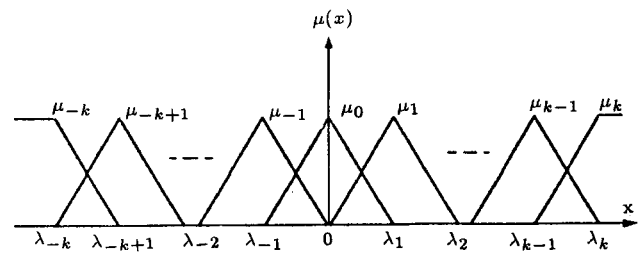

Figure 5. Membership functions.

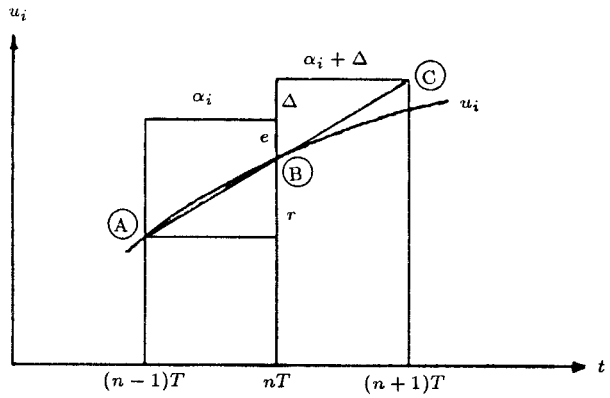

Figure 6. Linear prediction of u_i.

Structure of Fuzzy Rules

The input quantities of interest are the error and rate of change of interface inputs. Therefore, a two-premise and one-consequence structure is proposed. Consequently, the general form of the rules can be represented as follows:

If "error" is E_j and "rate" is R_l, Then "$\Delta\alpha_i$" is A_{l-j}.

The index of the members of output fuzzy set is obtained by subtracting the index of the members of the "error" from that of the "rate". For covering the total states which may occur, $J = 2k$ is required [5].

FUZZY INFERENCE

Assuming e and r as the input signals (the indexes are ignored for convenience), the inference for one subprocess can be formulated as follows.

Case I- Both e and r Are Within the Interval [-L,L]

It is obvious that any e (or r) intersects with two fuzzy sets E_i and E_{i+1} (or R_j and R_{j+1}). Therefore, only the following four fuzzy coordination rules are executed:

i. If "error" is E_{i+1} and "rate" is R_{j+1}, Then, "$\Delta\alpha$" is A_{j-i}.

ii. If "error" is E_{i+1} and "rate" is R_j, Then, "$\Delta\alpha$" is A_{j-i-1}.

iii. If "error" is E_i and "rate" is R_{j+1}, Then, "$\Delta\alpha$" is A_{j-i+1}.

iv. If "error" is E_i and "rate" is R_j, Then, "$\Delta\alpha$" is A_{j-i}.

The truth value or the degree of satisfaction of these rules is calculated by using the min-operator [6], i.e.,

$$\mu(i,j) = \min(\mu_i(e), \mu_j(r)). \tag{9}$$

If more than one output membership results, say μ_1 and μ_2, from executing two different fuzzy rules, Lukasiewicz fuzzy logic OR is used to get the combined membership function, μ, that is $\mu = \min(\mu_1 + \mu_2, 1)$. It should be noted that, in this problem, the combined membership is always the sum of the memberships, because the sum of the memberships being ORed is less than one.

Recall that the shapes of the membership functions of "$\Delta\alpha$" were required to be the same. Therefore, in the defuzzification process, the contribution from the members of "$\Delta\alpha$" in the THEN side of the fuzzy rules should be weighted by their memberships calculated from the IF side. Consequently, the crisp incremental output, $\Delta\alpha$, can be calculated by the following defuzzification algorithm:

$$\Delta\alpha = \frac{\sum \mu(i,j) \cdot \gamma_{j-i}}{\sum \mu(i,j)}, \quad \mu(i,j) \neq 0. \tag{10}$$

Figure 7 shows the input and output fuzzy sets for four coordination rules.

To determine the results of rules 1 to 4, consider eight possible regions as shown in Figure 8.

The outcomes of evaluating the min-operation for each premise of the fuzzy coordination rules, are illustrated in Table 1. After defuzzification, the following are obtained:

i. In regions R1, R2;

$$\Delta\alpha = \frac{[\mu_{j+1}(r)+\mu_i(e)]\cdot\gamma_{j-i}+\mu_j(r)\cdot\gamma_{j-i-1}+\mu_i(e)\cdot\gamma_{j-i+1}}{\mu_{j+1}(r)+\mu_j(r)+2\mu_i(e)},$$

ii. In regions R3, R4;

$$\Delta\alpha = \frac{[\mu_j(r)+\mu_{i+1}(e)]\cdot\gamma_{j-i}+\mu_j(r)\cdot\gamma_{j-i-1}+\mu_i(e)\cdot\gamma_{j-i+1}}{\mu_i(e)+\mu_{i+1}(e)+2\mu_j(r)},$$

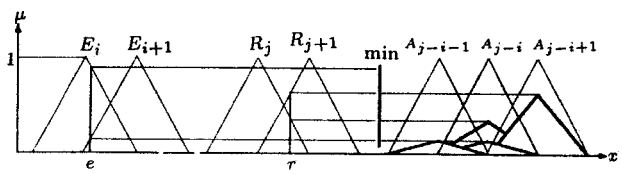

Figure 7. Output of execution rules 1 to 4.

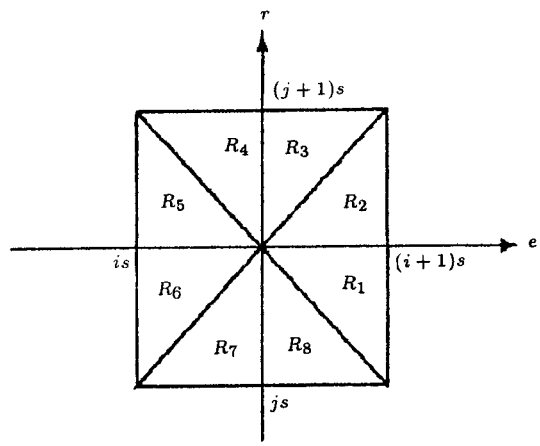

Figure 8. The eight possible regions (Case I).

Table 1. Result of evaluating the min-operations in rules 1 to 4.

Region	Rule 1 $\min(\mu_{i+1}(e), \mu_{j+1}(r))$	Rule 2 $\min(\mu_{i+1}(e), \mu_j(r))$	Rule 3 $\min(\mu_i(e), \mu_{j+1}(r))$	Rule 4 $\min(\mu_i(e), \mu_j(r))$
R1,R2	$\mu_{j+1}(r)$	$\mu_j(r)$	$\mu_i(e)$	$\mu_i(e)$
R3,R4	$\mu_{j+1}(e)$	$\mu_j(r)$	$\mu_i(e)$	$\mu_j(r)$
R5,R6	$\mu_{i+1}(e)$	$\mu_{i+1}(e)$	$\mu_{j+1}(r)$	$\mu_j(r)$
R7,R8	$\mu_{j+1}(r)$	$\mu_{i+1}(e)$	$\mu_{j+1}(r)$	$\mu_i(e)$

iii. In regions R5, R6;

$$\Delta\alpha = \frac{[\mu_j(r)+\mu_{i+1}(e)]\cdot\gamma_{j-i}+\mu_{i+1}(e)\cdot\gamma_{j-i-1}+\mu_{j+1}(r)\cdot\gamma_{j-i+1}}{\mu_j(r)+\mu_{j+1}(r)+2\mu_{i+1}(e)},$$

iv. In regions R7, R8;

$$\Delta\alpha = \frac{[\mu_{j+1}(r)+\mu_i(e)]\cdot\gamma_{j-i}+\mu_{j+1}(r)\cdot\gamma_{j-i+1}+\mu_{i+1}(e)\cdot\gamma_{j-i-1}}{\mu_{i+1}(e)+\mu_i(e)+2\mu_{j+1}(r)}.$$

Case II - Either e or r Is Outside the Interval [-L,L]

In this case, as shown in Figure 9, 12 possible regions exist. By using the same method described above, $\Delta\alpha$ can be analytically derived for each region. In R9 to R16 regions, only two fuzzy coordination rules are executed:

i. In regions R9, R10;
If "error" is E_k and "rate" is R_{j+1}, Then "$\Delta\alpha$" is A_{j+1-k}.
If "error" is E_k and "rate" is R_j, Then "$\Delta\alpha$" is A_{j-k}.

It is obvious that $\mu_j(r) + \mu_{j+1}(r) = 1$. Hence,

$$\Delta\alpha = \mu_{j+1}(r)\cdot\gamma_{j+1-k} + \mu_j(r)\cdot\gamma_{j-k}.$$

ii. In regions R11, R12;

$$\Delta\alpha = \mu_{i+1}(e)\cdot\gamma_{k-i+1} + \mu_i(e)\cdot\gamma_{k-i}.$$

iii. In regions R13, R14;

$$\Delta\alpha = \mu_{j+1}(r)\cdot\gamma_{j+k+1} + \mu_i(r)\cdot\gamma_{j+k}.$$

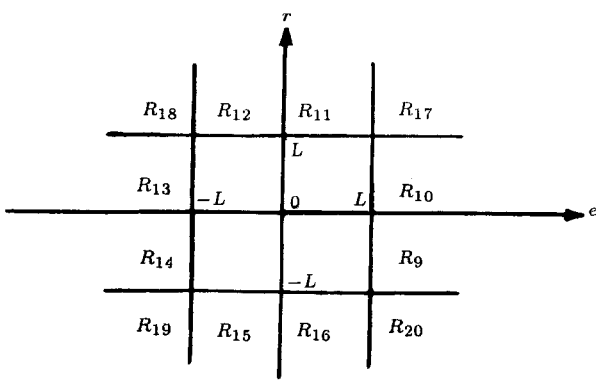

Figure 9. The 12 possible regions (Case II).

iv. In regions R15, R16;

$$\Delta\alpha = \mu_{i+1}(e)\cdot\gamma_{-k-i-1} + \mu_i(e)\cdot\gamma_{-k-i}.$$

In R17 to R20 regions, only one fuzzy coordination rule is executed:

i. in R17;
If "error" is E_K and "rate" is R_K, Then "$\Delta\alpha$" is A_0, hence; $\Delta\alpha = 0$.

ii. In R18; $\Delta\alpha = \gamma_{2k} = \gamma_J = H$.

iii. In R19; $\Delta\alpha = 0$.

iv. In R20; $\Delta\alpha = \gamma_{-2k} = \gamma_{-J} = -H$.

Finally, the crisp output of the fuzzy coordinator for the ith infimal controller, at sampling time nT, is calculated as:

$$\alpha_i(nT) = \hat{\alpha}_i(nT - T) + \Delta\alpha_i, \tag{11}$$

where $\Delta\alpha_i$ is the incremental output for ith controller, as given above. Since each infimal control problem is an FOC problem, the coordinator can send fuzzy coordination set $\tilde{\alpha}_i$ to the ith infimal control unit. The uncertainties on the crisp value of prediction, $\alpha_i(nT)$, can be included in the membership function, $\mu(\hat{\alpha}_i)$, as shown in Figure 4. ξ and η are the parameters which can be chosen by the experts, such that $\tilde{\alpha}_i$ would be near crisp and also cover the uncertainties. Finally, infimal control units solve an FOC problem and calculate $\hat{\alpha}_i(nT)$ and $\hat{m}_i(\alpha)$; control $\hat{m}(\alpha) = [\hat{m}_1(\alpha), \ldots, \hat{m}_n(\alpha)]$ is implemented to the process and $u_1(\alpha), \ldots, u_n(\alpha)$ will be the actual interface inputs.

CONCLUSIONS

Given the applicability of the interaction prediction principle, the supremal controller has the problem of predicting the interactions, comparing them with the actual one and updating the prediction to get an overall optimum.

It should be noted that the coordinator can also send the crisp value $\alpha_i(nT)$ rather than the fuzzy set $\tilde{\alpha}_i(nT)$. Therefore, the infimal control problem can be considered as an FOC or a conventional optimal control problem.

As demonstrated, the prediction is based on the interaction information of the present and last sample time. However, for better prediction, more information can be incorporated into the prediction algorithm using the previous data points. The analytical results can be obtained in an off-line form and are used in an on-line manner.

The described method may apply to every large scale system as well as truly complex phenomena, such as those founded predominantly in the social,economics and biological sciences. Actually, many hierarchical control systems with cohesive type interactions can be coordinated by the above scheme.

ACKNOWLEDGMENT

I would like to dedicate this paper to Professor Mesarovic, the father of "Large Scale Hierarchical Systems", in sincere appreciation of his kind cooperation and assistance during my academic association with him at Case Western Reserve University, USA, in the Fall of 1989, at which time I was privileged to attend a course presented by Professor Mesarovic, related to 'Abstract Systems Theory'.

REFERENCES

1. Mesarovic, M.D., Macko, D. and Takahara, Y., *Theory of Hierarchical Multilevel Systems*, Academic Press, New York, USA (1970).
2. Mesarovic, M.D., Takahara, Y., *Abstract Systems Theory*, Springer Verlag, Berlin, Heidelberg, Germany (1989).
3. Angelov, D.F.P. "Fuzzy optimal control", *Fuzzy Sets and Systems*, **47**, pp 151–156 (1992).
4. Luhanjula, M.K. "Fuzzy optimization: an appraisal", *Fuzzy Sets and Systems*, **30**, pp 257–282 (1989).
5. Ying, H. "A nonlinear fuzzy controller with linear control rules", *Automatica*, **29**(2), pp 499–505 (1993).
6. Zadeh, L.A., "Fuzzy Sets", *Information and Control*, **8**, pp 338–353 (1965).